Environmental Science
Processes & Impacts

PAPER

View Article Online
View Journal | View Issue

Cite this: *Environ. Sci.: Processes Impacts*, 2015, **17**, 1680

Oxygen profiling of the unsaturated zone using direct push drilling†

A. Sopilniak,[a] R. Elkayam,[ab] O. Lev*[a] and T. Elad*[a]

A methodology for oxygen profile measurements in the unsaturated zone is developed based on direct push drilling using sampling liners equipped with homemade silicone septa. The oxygen measurement is carried out by puncturing the septum with a commercial retractable optode needle fitted with a fluorescent tip. Metrological characteristics and method validation were carried out under laboratory conditions using different levels of oxygen and various water contents. The relative standard deviations under dry and water saturated soil conditions were less than 0.3% and 5% for 0.5 mg L^{-1} of oxygen and less than 2% and 3% for 9 mg L^{-1}. Field demonstrations in a calcareous-sandstone soil aquifer treatment system with a layered clayey, marl and sandstone lithology of widely different water contents provided down to 30 m deep profiles of the dissolved oxygen level with less than 1.5 m spatial resolution. A single sensor was used for over 50 field measurements, though recalibration was required after approximately 30 measurements due to the deterioration of the fluorescent tip.

Received 17th June 2015
Accepted 24th July 2015

DOI: 10.1039/c5em00270b

rsc.li/process-impacts

Environmental impact

Oxygen plays a major role in natural and engineered biological and chemical processes. Nevertheless, there is no satisfactory method for evaluating oxygen profiles as a function of depth in the vadose zone. In this study, we introduce a fast and reliable approach for oxygen depth profiling based on direct push drilling. The oxygen-depth profile was obtained for the first time from a 30 m vadose zone of a water recharge facility with a resolution of less than 1 m. This technique can be used to complement direct push drilling and can be applied to water saturated layers as well as to dry soils.

1. Introduction

The importance of dioxygen concentration in natural ecosystems as well as in engineered biological reactors cannot be overestimated. Changes in oxygen tension result in microbial population changes with different carbon fixation and mineralization pathways, rather than a mere change of process kinetics.[1,2] Therefore, oxygen is the most sought-after chemical profile in heterogeneous ecosystems as well as in unstirred technological reactors.[3–6]

Oxygen profiling in aqueous stratified streams, lakes and marine systems can be considered as a solved problem, though further improvements will always be sought.[7,8] Oxygen profiling in soil poses a different challenge and is much needed since the subsurface is often heterogeneous, and oxygen tension varies in time and space. The required spatial resolution of such measurements depends on the system and goes from the sub-mm scale for biofilms and biomats to a few centimeters in streambeds and can be of several decameters in unsaturated zone studies of marine and oceanic sediments. Soil gas measurements over contaminated sites containing non-aqueous phases can extend over an even larger scale up to many meters of soil.[9,10] Several techniques were developed to measure oxygen profiles over the different length scales using oxygen microelectrodes mounted on micro-translation stages for the sub-cm scale, fluorescent optical films[7] or an array of optodes[8] for the lower resolution range, and lander-type oxygen meters can be used to sample cores in the meter scale. Vertically nested sampling probes are used for low resolution soil gas profiling.[9–11] However, these techniques have only limited usefulness for oxygen profiling in the unsaturated zone. Molecular oxygen diffusion is over two orders of magnitude larger in the gas phase, and natural convection is also much faster. Currently, the most useful method for oxygen profiling of the unsaturated zone is to install several stationary water samplers or oxygen/redox sensors at different depths. Though these techniques provide time dependent information, they have limited spatial resolution, especially for deep locations, since a dedicated probe/sampler should be installed at each depth, and the sampling probes are not easily retrieved at the end of the measurement period.[12–18] Soil gas sampling techniques are impractical in moist or fine grained

[a]*Casali Center of Applied Chemistry, The Institute of Chemistry, The Hebrew University of Jerusalem, Jerusalem 91904, Israel. E-mail: ovadia@mail.huji.ac.il; alex.sopilniak@mail.huji.ac.il; Fax: +972 6586155; Tel: +972 6584191*

[b]*Wastewater Treatment & Reclamation Plant, SHAFDAN, Mekorot Israel National Water CO.LTD., Israel. E-mail: relkayam@mekorot.co.il; Tel: +972 3 9635113*

† Electronic supplementary information (ESI) available: Simulation of oxygen diffusion; oxygen sensing response time. See DOI: 10.1039/c5em00270b

soil.[9–11] We had to face the challenge of oxygen profiling during our studies of processes in the Shafdan effluent recharge systems, which will be described in more detail in the Experimental section. Briefly, the Shafdan system comprises a mechanical-biological domestic wastewater treatment followed by water recharge by surface spreading. The effluent infiltrates through some 30–40 m of the vadose zone to the aquifer and is reclaimed for irrigation a few hundred meters downstream. The most important parameter needed for gleaning the mechanism of such cleanup is still absent. The oxygen profile of the entire unsaturated zone of a water recharge facility has never been obtained, and only the upper few meters could be explored by stationary oxygen and redox probes.[19,20] Our own attempts to sample soil-gas were unsuccessful since the lithology involves layered clayey soil that is sometimes moist or even water saturated and does not allow gas sampling. We therefore developed an oxygen profiling approach based on direct push rigs using liners equipped with small rubber septa. The septa prevent oxygen contamination or release, and still the oxygen concentration can be determined soon after the liner withdrawal from the subsurface by puncturing the septum with an optical sensor enclosed in a protective metallic sleeve. Direct push rigs, often nicknamed after their inventing company Geoprobe™[21], produce boreholes by pushing a cylindrical liner into the subsurface. The liner filled with soil can then be pulled upwards. The equipment can be used to obtain continuous property profiles in unconsolidated soil materials and can be used to sample specific target locations by combining cone and push–pull drillings.[22–24] Several auxiliary geotechnical sensors were developed for direct push drilling, which allow obtaining continuous profiles of the lithostatic and hydrostatic pressures, electrical resistivity, seismic properties and even optical imaging.[25–27] However, devices for oxygen profiling have never been introduced, though the direct push rig equipped with a stainless steel screen permanent sampler is often used to obtain time dependent oxygen and redox data from specific depths.[28]

2. Materials and methods

2.1 Oxygen determination

Commercial liners equipped with home-made septa 1.5 mm in width were used to pull out soil cores, and the oxygen concentration was determined within one minute after the liner was withdrawn from the ground. Several 2 mm diameter holes were drilled in each liner (Fig. 1a). It was found preferable to drill the holes in opposite sides of the liner in order to minimize interference in case of detachment of a septum due to shear forces during the direct push drilling. Paper cylinders covered by Teflon bands were placed inside the liners to hold the viscous rubber in place, and then the holes were filled with silicone rubber (Elastosil E43, from PyroScience™) (Fig. 1b and c). The septa were left to dry for at least 24 hours. 2 mm septa were found optimal, since smaller septa were too rigid and detached from the liner when the optode was inserted, and larger septa were too loose and often detached from the liner during the direct push drilling. Careful cleaning of the inner section of the liner by pushing a cylinder wrapped with a cloth through the liner is essential to obtain a smooth inner surface and prevent peel off of the septa during drilling in coarse-grained soils. All in all, even with the optimized septa about 5% failure was encountered in our field tests.

Oxygen was measured using a commercial optode from PyroScience™ (OXR430), a retractable needle-type oxygen sensor, with a metallic shell of 1.1 mm in diameter and optical fiber of 430 μm in diameter (Fig. 2a). Optical oxygen sensing is based on red light excitation (610–630 nm) of fluorescent oxygen indicators and lifetime detection in the near infrared at 760–790 nm. Oxygen molecules quench the red signal and the concentration of oxygen is determined by the Stern–Volmer equation.[29] The sensor was calibrated by ambient and 0% oxygen levels (oxygen was depleted by using 3% wt Na_2SO_3). The specified absolute error of OXR430 is constant, 0.01 mg L^{-1} at 1% as well as at 20% O_2, corresponding to 9 and 0.5 mg L^{-1} of dissolved oxygen at 20 °C and atmospheric pressure.

2.1.1 Measurement procedure. Once in the field, the septa allow performing hermetically sealed measurements of oxygen in soil. The septa are punctured using the optode metallic shell and the fiber is inserted into the soil core (Fig. 2b). The signal is allowed to stabilize for a few seconds before taking stationary readings.

2.2 Method testing

The sensing method was tested in the laboratory on a simulation system consisting of a 20 cm PVC liner blocked by inlet and outlet caps at its two ends and equipped with metal valves for gas inlets – two at the top for different gases and one at the bottom. A schematic depiction of the simulation setup is shown in Fig. 3a. Several 2 mm septa were fixed along the liner's wall,

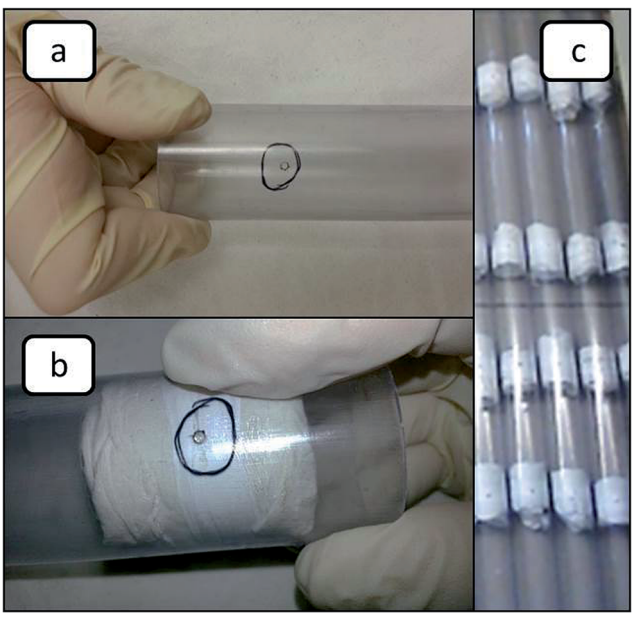

Fig. 1 Septum preparation: (a) 2 mm hole drilled in a PVC liner (circled). (b) Filling the hole with silicone rubber RTV-1 E-43. (c) Septa equipped liners during the drying stage with inner Teflon bands to hold the wet RTV rubber in place. The bands are removed after drying.

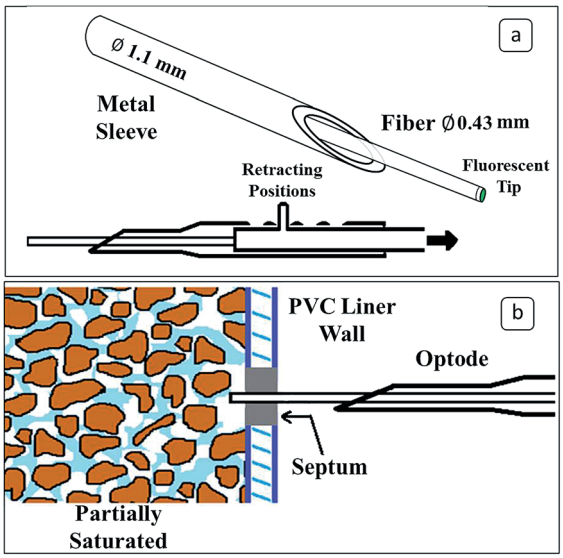

Fig. 2 (a) Retractable needle-type oxygen sensor. The fiber can be moved to one of the four positions, up to 12 mm from the sleeve sensing with direct soil contact. An optode pierces through the silicone septum in the PVC liner wall of the Geoprobe™ tubing and reaches the soil.

and a sensor spot (OXSP5, PyroScience™) and a spot adapter (SPADBAS, PyroScience™) were glued to the liner's inner and outer walls, respectively, which served as an unbiased fixed reference. Three cases were tested.

First, to simulate dry soil (0% saturation), the liner was filled with dry sand (>90% sandy soil), and then flushed with air and nitrogen at different ratios in order to obtain a range of oxygen concentrations. The sand was shaken after the flow of air and nitrogen was stopped in order to ensure uniform oxygen distribution inside the liner.

Secondly, to simulate measurements in saturated soil (100% saturation, corresponding to 26% wt water), the liner was first filled with tap water. Sand was then added, keeping the upper part of the column full of water and free of sand. Nitrogen was bubbled into the top of the water column until the desired oxygen concentration was reached, and then the soil filled section of the column was flushed with water, leaving only a few mm of a water head above the soil surface. Reference oxygen measurements, unbiased by the septa, were established by measuring the oxygen concentration in the top of the water column by using an OXR430 sensor.

Thirdly, to simulate measurements in semi-saturated soil (50% saturation, corresponding to 13% wt water), the liner was filled with tap water and sand as before. The water was let to drain, and then different concentrations of air and nitrogen mix were made to flow through the liner. In each test concentration, a reference measurement was carried out by using the stationary spot sensor, and compared to three test measurements using the OXR430 retractable needle-type minisensor and the three septa as described above.

2.3 Oxygen penetration through the soil core

Under field operation, the sampled soil core may be contaminated with atmospheric oxygen from the two ends of the liner. The process of liner retrieval exposes the liner to air through the top and bottom ends of the liner. Moreover, the bottom side of

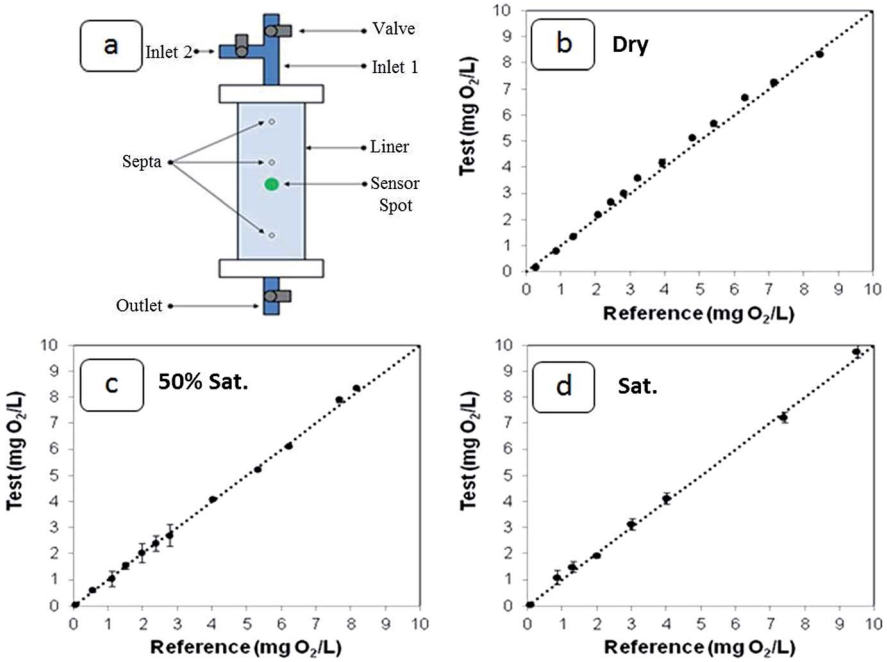

Fig. 3 (a) A schematic description of the oxygen measurement test system. (b–d) Test *versus* reference stationary oxygen measurements in dry (b), 50% v/v water content (c), and saturated (d) sand. Correlation was 0.995, 0.999 and 0.997, respectively. Dotted lines represent the 1 : 1 line. Bars represent the standard error of three different test measurements through three different septa. Bars are often smaller than the symbols.

the liner may be contaminated by oxygen from the beginning of the pull-up process until the time that it is capped, and the septum is punctured by the optode. In addition, the soil at the top side of the liner is exposed to the atmosphere also during the time period between the removal of the previous liner from the ground and the pull out of the current liner, which affects the upper part of the soil in the liner itself. Oxygen contamination through the septa was ruled out by mathematical simulations showing negligible penetration of oxygen through the RTV septum. A full description is provided in the ESI.†

The period of penetration of oxygen to the top side can be shortened by insertion of a cork in the lower side of the liner. The cork slides up along the liner as it is filled by the soil, keeps the upper part of the liner plugged and prevents oxygen contamination during the pull up-process. However, this solves only part of the problem, since the soil is still exposed to oxygen during the time interval between the extraction of the previous liner and the time the cork starts to slide up along the next liner. The oxygen penetration depth should be shorter than the distance between the septum and the nearest end of the liner. Oxygen penetration tests were carried out with dry sand to represent the worst case of fastest oxygen penetration conditions.

Sand has high porosity[30,31] and dry conditions leave the soil voids available for fast oxygen penetration. To this end, we fixed an oxygen sensor spot in the middle of a 1.5 m liner and filled the liner with dry sand and then thoroughly flushed the sand with nitrogen. Then, we removed the inlet cover, letting ambient air diffuse freely into the liner and recorded the oxygen level as a function of time at a fixed spot. Liners filled with soil to different levels above the oxygen sensor were used to measure the time for oxygen penetration to different depths. Data collection began with nitrogen flushing.

2.4 Field research area

Field studies were carried out in the Shafdan water recharge lagoons. The Shafdan wastewater treatment plant treats 130 Mm^3 of predominantly domestic wastewater per year and serves a population of 2 million people in the Tel Aviv Metropolitan Area. The process includes conventional mechanical-biological treatment and surface spreading effluent recharge. The infiltration lagoons are flooded for one day by the Shafdan effluent, and the lagoons are then allowed to dry for 2–3 days. The water infiltrates through 30–40 m of the unsaturated zone and then flows horizontally in the saturated zone for 6–36 months before being reclaimed for irrigation. The Shafdan recharge area is located in the coastal aquifer which supplies 20% of Israel's potable water. The coastal aquifer, a Pliocene-Pleistocene phreatic aquifer located along the Mediterranean Sea coast, is predominantly calcareous sandstone interlaced by intercalations of clay, silt and loam layers. It overlies impermeable shales of the Saqiye group at a depth of *ca.* 100–150 m below ground level.

Core soil collection was performed in a percolation lagoon, 24 and 48 hours after the field flooding ended. The sampling was done by using direct Push VTR 9700 machinery from AMS Technologies™. The rig pushes PVC liners of 3.8 cm in diameter and 1.5 m long. The core is then retrieved full of soil to the surface. Sampling was done down to 30 meters below the ground.

2.5 Water content determination

The soil water content was determined by a standard method of loss on ignition (LOI), in which soil samples are weighed before and after heat treatment at 105 °C for at least 24 h.[32] The volumetric water content is derived from additional measurements of soil density done while the soil is still within the liner.[33]

3. Results and discussion

3.1 Validation of the oxygen analysis

Validation of the oxygen determination methodology was carried out using the constructed setup shown in Fig. 3a by comparing oxygen sensing through the rubber septa with the signal of the stationary optode. Data were collected for dry, under-saturated (50% v/v) and saturated (100% v/v) coarse sandy soil to closely represent the coastal region of the research area. Sands with different water contents were equilibrated with different ratios of air and nitrogen to represent a wide range of oxygen concentrations. Immediately after gas flow was stopped, the system was hermetically sealed. Then, the three septa were punctured and oxygen levels were measured inside the sand using our optode. Reference measurements with a stationary optode were taken before applying our measurement methodology and after.

Fig. 3b–d depict the fits of the measured oxygen levels by our methodology and the response of a stationary optode that was not biased by the septa for three water contents. Each test was carried out three times using a different septum for each measurement. In all cases, a good fit was obtained between the unbiased stationary reading and the proposed method. The relative standard deviation, a measure of precision, was less than 5%, and it was practically independent of the oxygen level and the water content. The absolute bias of the test was always lower than 0.2 mg L^{-1} of oxygen.

The curves in Fig. 3b–d depict the measurements through the septa and by the reference stationary optode. The linear 1 : 1 correlation coefficients were found to be 0.995, 0.999 and 0.997 for 0%, 50% and 100% water saturation content, respectively.

The relative standard deviation was less than 3% over the entire oxygen range. The relative bias (*i.e.* maximal difference between a measurement through a septum and the stationary optode) increased to 5% at low oxygen concentrations (0.5 mg L^{-1}) under the under-saturated as well as under the saturated conditions.

3.2 Oxygen penetration depth

Oxygen penetration depth evaluation was conducted using dry soil as described in the Experimental section. First, the response time of the sensor itself was evaluated as a function of the water content. The dynamic response of the sensor from its penetration through the septum to the stabilization of the response is depicted in Fig. S3# in the ESI.† Although the response time was larger in dry sand than in the 50% wetted

soil, the sensor stabilized within a few seconds in both cases. Thus, the sensor response rate, which is of the order of seconds, does not bias the determination of the much slower oxygen penetration rate into the soil.

The time required for oxygen to penetrate a specific depth was measured for several different liners, as described in the Experimental section. A 1.5 m liner was filled with sand and flushed with nitrogen until the oxygen level dropped to 0 at a stationary sensor located at the middle of the liner. The liner was then sealed hermetically and left to stand for 24 h to ensure zero oxygen leakage. The upper cap of the liner was then removed and oxygen was continuously monitored. This process was done for 7 different lengths between the sensor and the upper edge, ranging from 10 to 75 cm. Measurements were carried out at 25 ± 1 °C and 695 ± 2 Torr. Fig. 4 depicts the response of the sensor at seven different levels below the upper edge of the soil in the liner after the cap was removed from the liner. In all cases, the readings were initially 0 mg L^{-1} until an oxygen breakthrough was reached and the oxygen signal increased exponentially. As expected, longer paths induced longer breakthrough periods. The oxygen levels were monitored up to 1 mg L^{-1} of oxygen. Eqn (1)–(3) describe the theoretical oxygen concentration (C) as a function of time (t) from the beginning of the exposure of the soil to oxygen and the distance (x) between the top of the soil and the sensor, $C(x, t)$.

$$C(x,t) = C_0 \operatorname{erfc}\left(\frac{x}{2\sqrt{\frac{D_0 \Phi^2 \left(\frac{\varepsilon_g}{\Phi}\right)^{\tau} t}{\varepsilon_g + B\theta_v}}}\right) \quad (1)$$

$$\tau = \frac{\log\left(\frac{2\varepsilon_g{}^2 + 0.04\varepsilon_g}{\Phi^2}\right)}{\log\left(\frac{\varepsilon_g}{\Phi}\right)} \quad (2)$$

Eqn (1) is a one-dimensional solution of the Fickian diffusion equation modified for soil porosity and water content.[34,35] Eqn (2) gives the tortuosity according to the three-porosity-model.[36,37] The notations are defined in Table 1. Under dry conditions, the porosity ε_g approaches the soil total porosity Φ and the volumetric water content θ_v equals zero, thus eqn (1) turns into:

$$C(x,t) = C_0 \operatorname{erfc}\left(\frac{x}{2\sqrt{D_0 \Phi t}}\right) \quad (3)$$

The parameters used for generating the theoretical curves were all either based on literature values (*e.g.* D_0, C_0, B) or on experimental values obtained by independent measurements of our set-up (Φ, ε_g, θ_v). The fit shown in Fig. 4 (upper) between theory and practice is remarkable and it is achieved without using any adjustable parameter. In fact, when we used the porosity as an adjustable parameter to receive a best fit between theory and practice we obtained 0.369 ± 5% instead of 0.3640 ± 5% which was determined by gravimetry[38] for dry sandy soil. These values are well within the estimated errors.

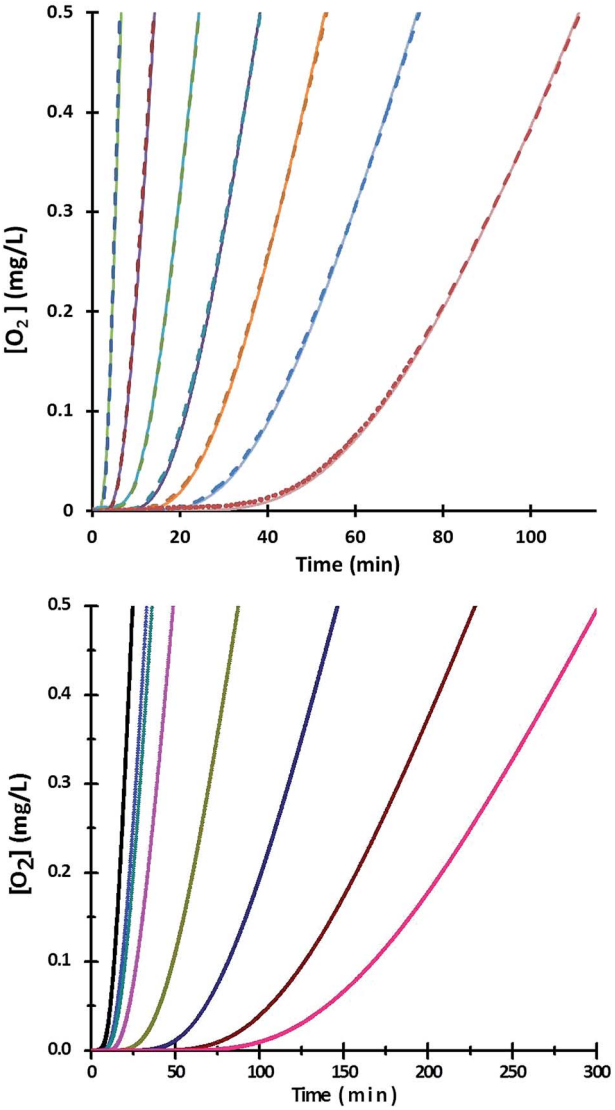

Fig. 4 (Upper) Oxygen breakthrough curves at seven different distances (10, 20, 30, 40, 50, 60, and 75 cm, from left) from the edge of the liner. Solid curves calculated by eqn (3), and the dashed lines are experimental time traces. The experiment was done under 47.5% relative humidity and 25 °C. (Bottom) Theoretical breakthrough curves calculated for the parameters of Table 1 and 0%, 5%, 10%, 25%, 50%, 70%, 90% and 100% (from left) water soil saturation. x = 30 cm.

Fig. 4 (bottom) depicts the breakthrough curves for 0%, 5%, 10%, 25%, 50%, 70%, 90% and 100% volumetric water saturation. Higher water content slows oxygen penetration into the soil, and thus dry conditions are the worst case scenario for ambient oxygen contamination. For example, taking 20 minutes as a reasonable time for completing a field test, *i.e.* the time of exposure of the edge of the soil to ambient oxygen, and using a threshold oxygen level of 0.1 mg L^{-1} (as the minimum method detection limit) gives penetration depths of 35, 31, 29, 25, 19, 15, 12, and 10 cm after 20 minutes for 0, 5, 10, 25, 50, 70, 90 and 100% volumetric water saturation, respectively. For the case of

Table 1 Definitions of the notations and their experimental[a] or literature values under the laboratory test conditions

Symbols	Definition and units	Values	Remarks
$C(x, t)^{\dagger}$	Oxygen concentration as a function of distance and time		Calculated
C_0	Concentration of oxygen in equilibrium with atmospheric oxygen (mg L^{-1})	8.0 ± 0.1 (mg L^{-1})	Battino R. *et al.*[39]
x	Distance from the liner edge (cm)	$10 \leq x \geq 75$ cm	This study
$t^{\ddagger}$	Time (s)		This study
B	Bunsen's coefficient of solubility	6.42×10^{-3}	Weiss R. F.[40]
θ_v	Volumetric water content	$0\% < \theta_v < 36\%$	This study
D_0	Oxygen diffusion coefficient (cm^2 s^{-1})	0.23 ± 0.01 (cm^2 s^{-1})	Astrath N. *et al.*[41]
Φ	Soil total porosity	0.36 ± 0.02	This study
ε_g	Air-filled porosity	$0 < \varepsilon_g < \Phi$	This study
τ	Tortuosity	For 0–50% saturation $1 < \tau < 3$	Calculated by eqn (2)

[a] All measurements were carried out at 695 ± 2 Torr, 25 ± 1 °C and a relative humidity of 47.5 ± 0.5%. [†]Initial conditions of $C(x, t = 0) = 0$; boundary conditions: $C(x = 0, t) = 0$; $C(x = \infty, t) = C_0$. [‡]Recorded every second.

the percolation lagoons of the Shafdan, the average volumetric water content is *ca.* 10%, and thus the distance from the closest septum to the bottom and top edges of the liners was set to 30 cm, calculated for 20 minutes of oxygen exposure.

The retractable needle-type optode combined with the Geoprobe™ liner modification with installed septa shows a response time within seconds for soil-oxygen measurements. This result is faster than many other methods relying on optical arrays and films[7,8,13,17] and is suitable for in field direct measurements, unlike methods based on diffusion cells,[10,12,42] which are better for longer time scales (hours to days). The methodology described in this study has increased the vertical resolution and reachable depth for dissolved oxygen measurements and other oxygen sensitive water quality parameters, for which miniature sensing devices exist.

3.3 Field results

3.3.1 Water content and lithology. The lithology at the site is described in Fig. 5a. The calcareous sandstone lithology is interrupted by clayey layers of lower hydraulic permeability[31] at around −8.5, −12.5, −16 and −22 m. The water content profile was determined on two consecutive days. The results are expressed as % wt/wt and % v/v and presented in the same figure (Fig. 5b and d). The water content profile was determined at a resolution of 75 cm, though it is expressed as a continuous line. The water content profile which was determined 24 hours after flooding shows peak water contents at the top soil and above −9 and −12.5 m and around −16 m corresponding to the hydraulic clayey barriers at these points. The water content results agree well with our visual field observations of water saturation. The day-to-day changes of the water contents are larger at the upper half of the profile and show depletion of the high water content in the top soil due to water infiltration, and accumulation of water above the −9 m clayey barrier. At deeper locations, a downward progress of the high water content layer from −15 to −16 m can be observed.

3.3.2 Oxygen profile as a function of depth. Oxygen profiles were evaluated in the field, 24 and 48 h after the beginning of the flooding session and the observed profiles are depicted in Fig. 5c and e.

In both cases, two distinguished zones can be observed: an oxygenated (aerobic) zone, located from the surface to *ca.* 10–12 m, and an anaerobic zone from *ca.* 10 m downward. The data points were reported only if two measurements through two different septa gave identical results within less than 0.1 mg L^{-1}. This was achievable despite the heterogeneity of the soil and the variability of the oxygen concentration.

On day 1, we witnessed a steep decline of oxygen concentration from near saturation, 8.1 mg O_2/L at the surface, corresponding to an ambient temperature of 26 ± 2 °C and 760 Torr, to 3.9 mg L^{-1} at *ca.* −1.5 m. A slight O_2 increase is then observed between −1.5 and −2.5 m followed by a plateau at 4.3 mg L^{-1} down to −7 m. A sharp decrease of the oxygen level is then observed between −7 and −10 m, at the end of which oxygen drops to zero.

On the second day, atmospheric oxygen penetrated from the surface and the oxygen level in the region −1.5 to −5 m exhibited a gentle decrease from 6.1 to 5.5 mg L^{-1}. This level is substantially higher than the level of 4.3 mg L^{-1} on day 1. Oxygen was depleted on day 2 only at −12 m and the oxygen decrease was less steep compared to day 1. On both days, the level of oxygen below −12 m was 0 except for two points, −30 m on the first day and −15 m on day 2. In the first case, the retrieval of the liner to the surface took more than 40 minutes and in the second case, the delay time between the retrieval of the last liner (for depth −28.5–30) was also excessive (above 50 minutes); thus in both cases oxygen diffusion likely reached the septa before the measurement took place (see Sections 2.3 and 3.1).

Explanation of the complex oxygen profiles. In order to understand the oxygen profile in the upper 7 m of the subsoil, we have to recall some key points. First, water is introduced into the upper 7 m rather quickly during the flooding phase when the lagoon is still full of water. During this phase oxygen penetration into the subsoil is slow, since oxygen can be carried downwards only by the convection of the water phase.

Second, the top soil is rich with organics and biofilms[19,43] and a natural gradient of organic matter and bacteria is developed from the top soil downwards due to sieving and adsorption mechanisms. Thus, the initial drop in oxygen in the first 1.5 m can be explained by a fast biodegradation due to the high concentrations of organic matter and the abundance of bacteria

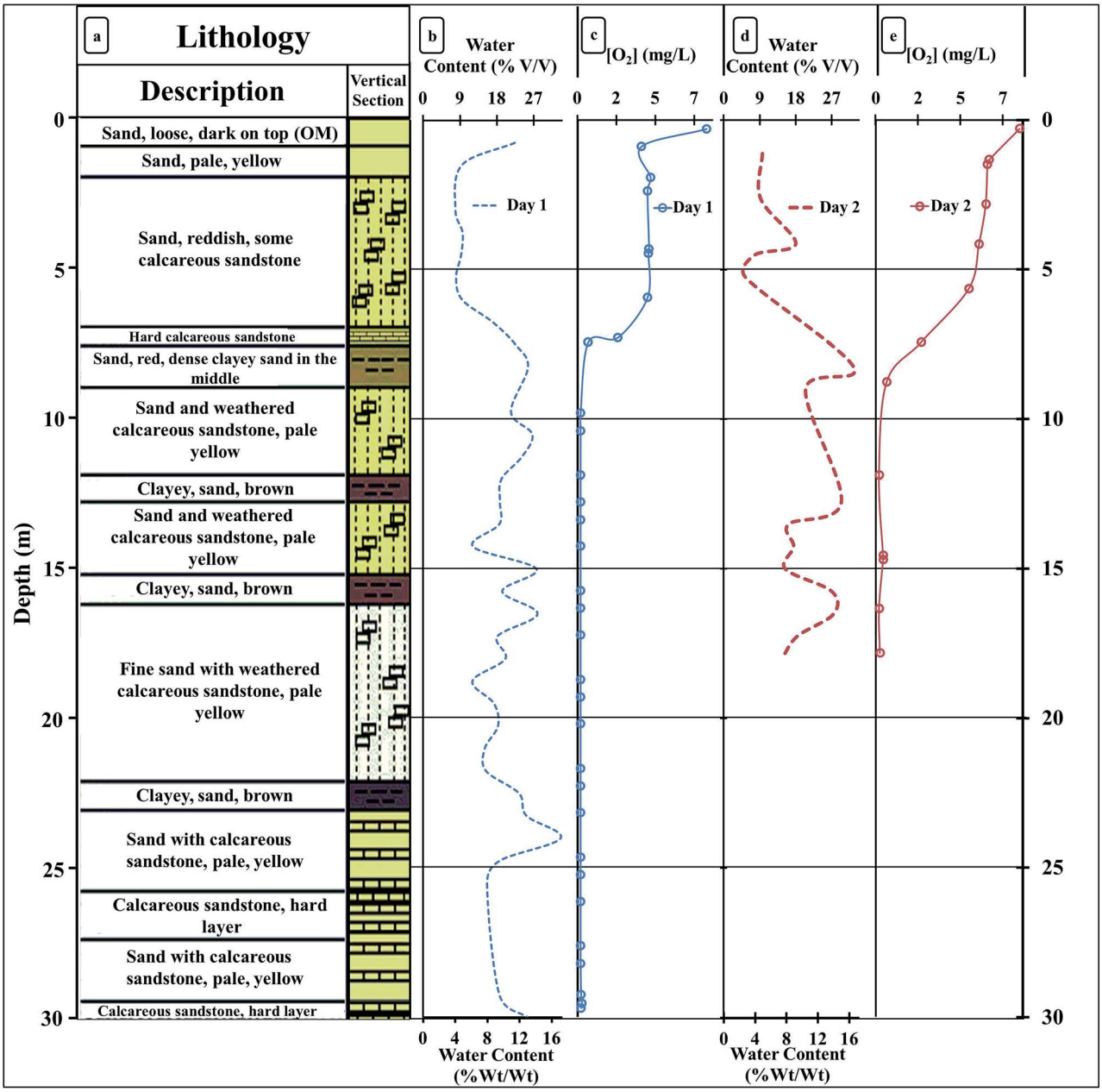

Fig. 5 Field results from Yavne 2 percolation lagoon: (a) lithology profile of the percolation lagoon up till 30 m. The soil consists mostly of sand and calcareous sandstones with interlayers of clayey soil at −8.5, −12.5, −16 and −22 m. (b) Water content as a function of soil depth depicted as % wt/wt and % v/v of day 1 – 24 hours after flooding. (c) Oxygen profile as a function of depth taken on day 1. (d) Water content as a function of soil depth depicted as % wt/wt and % v/v on day 2 – 48 hours after flooding. (e) Oxygen profile as a function of depth taken on day 2.

in the top soil. It is also possible that some of the observed attributes of the oxygen profile stem from the high heterogeneity of the soil.

The small rise in oxygen which is observed between *ca.* −1.5 and −2.5 m is attributed to the decreased amount of bacteria in the deeper layers which slows oxygen consumption and to high oxygen penetration during the drying phase. The plateau at −2.5 to −7 m results from a balance between oxygen penetration in the gas phase and oxygen demand for biodegradation, with water seepage downward playing an additional minor role. In the bottom section from −7 to *ca.* −10 m, there is a steep decrease in oxygen. This is largely attributed to the accumulation of saturated layers in and above the clayey layer (Fig. 5a). The hydraulic barrier decreases the void fraction, the gas phase is decreased accordingly and oxygen flux downwards being sustained only by water convection and dissolved gas diffusion. Since biodegradation continues due to the large level of organic matter, the oxygen level steeply drops to zero.

The main features of the oxygen profile on the second day are similar to those obtained on day 1 with some differences that can be attributed to the water convection downwards during the passing day and to oxygen penetration from the surface through

the increasing void fraction which was still largely occupied by water on day 1. Thus, the increase of the oxygen level between 0 and −1.5 m is attributed to oxygen penetration from the atmosphere during the additional 24 hours of drying.

The moderate decline in the oxygen level on day 2 compared to the plateau of day 1 is due to the increased path-length required for oxygen penetration from the surface. The sharp decline of the oxygen level (between −7 and −10 m) is less steep on day 2 due to oxygen containing water seepage to the layer of saturated water that accumulated above the clayey barrier. Water convection from the clayey layer downward is also responsible for the expansion of the aerobic zone on day two (extending down to −12 m).

4. Conclusions

A new approach for measuring oxygen was devised, validated under laboratory tests and demonstrated under complex conditions by field studies. The used direct push–pull drilling technique can be complemented by relatively simple auxiliaries that allow oxygen profile measurements in the field. The field tests which were carried out on two consecutive days showed consistency with the physical parameters of the researched unsaturated zone. The limitations of the proposed approach were also underscored in this study. Oxygen profiling is limited to approximately 30 m by the length of time that it takes to pull up the filled liners. Despite this limitation, we believe that the process can be extended to the measurements of other ambient air sensitive parameters such as redox potential, hydrogen sulfide, reduced sulphur species, ammonia and nitrogen for which miniature electrochemical and optical sensors have already been developed.

Acknowledgements

The authors acknowledge the help of Mekorot Ltd and the financial help of the scientific infrastructure program of the Ministry of Science and the financial help of the National Water Authority. AS thankfully acknowledges a Teva Ltd doctoral scholarship.

References

1 C. S. Foote, *Active Oxygen in Chemistry*, Blackie Academic & Professional, 1st edn, 1995.
2 H. Decker and K. E. van Holde, *Oxygen and the Evolution of Life*, Springer, Berlin, Heidelberg, 1st edn, 2010.
3 J. Gli'nski and W. Stepniewski, *Soil Aeration and its Role for Plants*, CRC Press, 1st edn, 1985.
4 C. Baleizã, S. Nagl, M. Schäferling, M. N. Berberan-Santos and O. S. Wolfbeis, *Anal. Chem.*, 2008, **80**, 6449–6457.
5 H. Suzuki, *Electroanalysis*, 2000, **12**, 703–715.
6 R. N. Glud, *Mar. Biol. Res.*, 2008, **4**, 243–289.
7 M. Vieweg, N. Trauth, J. H. Fleckenstein and C. Schmidt, *Environ. Sci. Technol.*, 2013, **47**, 9858–9865.
8 L. F. Rickelt, L. Askaer, E. Walpersdorf, B. Elberling, R. N. Glud and M. Kühl, *J. Environ. Qual.*, 2013, **42**, 1267–1273.
9 L. H. Wilson, P. C. Johnson and J. R. Rocco, *Collecting and Interpreting Soil Gas Samples from the Vadose Zone*, 2005.
10 M. Clark, S. Jarvis and E. Maltby, *Commun. Soil Sci. Plant Anal.*, 2001, **32**, 369–377.
11 B. M. Patterson and G. B. Davis, *Ground Water Monit. Rem.*, 2008, **28**, 68–74.
12 W. H. Patrick, *Soil Sci. Soc. Am. J.*, 1977, **41**, 651–652.
13 G. Holst, R. N. Glud, M. Kühl and I. Klimant, *Sens. Actuators, B*, 1997, **38**, 122–129.
14 I. Klimant, G. Holst, O. Kohls, V. Meyer and J. K. Gundersen, *Science*, 1999, **46**, 1–2.
15 G. C. Topp, B. Dow, M. Edwards, E. G. Gregorich, W. E. Curnoe and F. J. Cook, *Can. J. Soil Sci.*, 2000, **80**, 33–41.
16 A. Schwen, J. Böttcher, C. von der Heide, T. Fandré, M. Deurer and W. H. M. Duijnisveld, *Soil Sci. Soc. Am. J.*, 2011, **75**, 813–821.
17 H. Hecht and M. Kölling, *Sens. Actuators, B*, 2001, **81**, 76–82.
18 J. P. Fischer and K. Koop-Jakobsen, *Sens. Actuators, B*, 2012, **168**, 354–359.
19 E. Idelovitch and M. Michail, *Water Environ. Fed.*, 1984, vol. 56, pp. 936–943.
20 B. Herman and E. Idelovitch, *J. Irrig. Drain. Div., Am. Soc. Civ. Eng.*, 1987, **113**, 516–535.
21 Direct Push Series Drilling Machines, http://geoprobe.com/direct-push-series-drilling-machines, accessed June 2015.
22 N. Tillman and L. Leonard, *Vehicle Mounted Direct Push Systems, Sampling Tools and Case Histories: An Overview of an Emerging Technology*, 1993.
23 J. A. Jacobs, M. Kram and S. Lieberman, in *Standard Handbook of Environmental Science, Health, and Technology*, ed. J. Lehr, McGraw-Hill, New York, 2000, pp. 151–163.
24 V. A. Zlotnik, M. Burbach, J. Swinehart, D. Bennett, S. C. Fritz, D. B. Loope and F. Olaguera, *Environ. Eng. Geosci.*, 2007, **13**, 205–216.
25 J. J. Butler, J. M. Healey, G. W. McCall, E. J. Garnett and S. P. Loheide, *Ground Water*, 2002, **40**, 25–36.
26 W. McCall, J. J. Butler, J. M. Healey, A. A. Lanier, S. M. Sellwood and E. J. Garnett, *Environ. Eng. Geosci.*, 2002, **8**, 75–84.
27 Geotechnical Sensors, http://clu-in.org/characterization/technologies/dpgeotech.cfm, accessed June 2015.
28 M. K. Schulmeister, J. M. Healey, J. J. Butler and G. W. McCall, *J. Contam. Hydrol.*, 2004, **69**, 215–232.
29 C. Mcdonagh, C. Kolle, A. K. Mcevoy, D. L. Dowling, A. A. Cafolla, S. J. Cullen and B. D. MacCraith, *Sens. Actuators, B*, 2001, **74**, 124–130.
30 A. R. Freeze and J. A. Cherry, in *Groundwater*, Prentice-Hall, 1st edn, 1979.
31 K. M. Hiscock, *Hydrogeology Principles and Practice*, Wiley-Blackwell Publishing, 1st edn, 2005.
32 M. Pansu and J. Gautheyrou, in *Handbook of Soil Analysis*, Springer, Berlin, Heidelberg, 2006, pp. 3–13.
33 R. Lal and M. K. Shukla, *Principles of Soil Physics*, Marcel Dekker inc., 1st edn, 2004.
34 G. H. Bolt and M. G. Bruggenwert, in *Soil Chemistry: Basic Elements*, Elsevier Science Ltd, 2nd edn, 1976, pp. 213–220.
35 G. L. Guymon, *Water Resour. Res.*, 1970, **6**, 204–210.

36 P. Moldrup, T. Olesen and S. Yoshikawa, *Soil Sci. Soc. Am. J.*, 2004, **68**, 750–759.
37 P. Moldrup, T. Olesen, P. Schjonning, T. Yamaguchi and D. E. Rolston, *Soil Sci. Soc. Am. J.*, 2000, **64**, 94–100.
38 C. Dirksen, *Soil Physics Measurements*, Catena Verlag GMBH, Reiskirchen, Germany, 1st edn, 1999.
39 R. Battino, T. R. Rettich and T. Tominaga, *J. Phys. Chem. Ref. Data*, 1983, **12**, 163–177.
40 R. F. Weiss, *Deep-Sea Res. Oceanogr. Abstr.*, 1970, **17**, 721–735.
41 N. G. C. Astrath, J. Shen, D. Song, J. H. Rohling, F. B. G. Astrath, J. Zhou, T. Navessin, Z. S. S. Liu, C. E. Gu and X. Zhao, *J. Phys. Chem. B*, 2009, **113**, 8369–8374.
42 P. Holter, *Soil Biol. Biochem.*, 1990, **22**, 995–997.
43 B. E. Rittmann, *Water Resour. Res.*, 1993, **29**, 2195–2202.